# CAPABILITY OF AUTOLOGOUS PLATELET RICH PLASMA TO ALLEVIATE EXPERIMENTALLY INDUCED DIABETIC NEPHROPATHY IN ADULT MALE ALBINO RAT (LIGHT AND ELECTRON MICROSCOPIC STUDY)

*Enas Anwar Bekheet*

Anatomy and Embryology Department, Faculty of Medicine, Ain Shams University, Cairo, Egypt.

**Corresponding author**:
Enas Anwar Bekheet
Mobile: 01224037554
**e.mail:**
eno.anatomy@yahoo.com.

Received: 19/9/2023
Accepted: 8/10/2023
**Online ISSN: 2735-3540**

## ABSTRACT:

***Background:*** *Diabetic nephropathy is a common complication of diabetes. In prior studies platelet-rich plasma (prp) ameliorated diabetic cardiac injury and diabetic neuropathy.*

***Aim of the work:*** *This work aimed to evaluate the capability of autologous platelet-rich plasma to alleviate experimentally induced diabetic nephropathy in adult male albino rat.*

***Material and methods:*** *Forty adult male albino rats were used in this study. Rats were distributed into equal four groups.*

***Group I (control):*** *rats were redistributed into two equal subgroups:*

*- Subgroup a: rats received no treatment for six weeks.*

*- Subgroup b: each rat was intraperitonially injected by a single dose of citrate buffer (1ml) then kept without any treatment for six weeks.*

***Group II (diabetes):*** *each rat received 0.5 mL/kg prp, twice weekly by subcutaneous injection for six weeks.*

***Group III (prp):*** *each rat received a single intraperitoneal injection of 55mg/kg Streptozotocin (Sz), then after confirmation of diabetes they kept without any treatment for six weeks.*

***Group IV (diabetes+ prp):*** *each rat received a single intraperitoneal injection of Sz as in group III and from the day of confirmation of diabetes, prp was injected as in group II.*

***Results:*** *The diabetic group showed that the cells of the renal tubules were having cytoplasmic vacuoles with scanty apical microvilli and scanty basal mitochondria. Meanwhile, the renal corpuscles showed hypertrophied glomeruli and enlarged mesangial cells. Diabetic rats that received prp showed nearly intact renal tubules and renal corpuscles.*

***Conclusion****: Autologous platelet rich plasma could alleviate the histological changes of diabetic nephropathy in adult male albino rats.*

***Keywords:*** *Diabetic Nephropathy, Platelet Rich Plasma, Diabetes.*

## INTRODUCTION:

Diabetes is the most prevalent chronic metabolic disorder which is marked by elevated level of blood glucose. Hyperglycemia occurs with diabetes as a result of reduction of insulin secretion from the pancreas and/or peripheral insulin resistance. In consequence to enduring hyperglycemia, cells damage occurs through glucose oxidation, glycation, and nitric oxide release leading to harmful impacts on different body organs such as kidneys, retina and heart. Regarding the kidneys, it promotes diabetic nephropathy “a chief reason of morbidity among diabetic patients”. About

50% of patients with type II diabetes and one third with type I diabetes develop diabetic nephropathy ten to twenty years from its inception. The mechanisms by which diabetic nephropathy occur include inflammation, oxidative stress and hemodynamic disturbance [1-5].

Platelet-rich plasma (prp) is considered a new by-product of blood in regenerative medicine, thanks to its part in tissue repair and healing by activating the stem cells. It differs from blood plasma in having a high concentration of platelets. Platelets carry more than eight hundreds of different proteins in their α-granules and multiple growth factors required for the healing process such as, endothelial growth factor and platelet-derived growth factors [6-8].

Platelet-rich plasma is considered cheap, easy to obtain with no risk of rejection in autologous form. Additionally, in prior studies it ameliorated diabetic cardiac injury, diabetic neuropathy and gamma radiation induced nephrotoxicity in rats by decreasing tissue inflammation, modulating oxidative damage and cellular apoptosis [9-11]. Hence, this study was mapped out to evaluate the capability of prp to alleviate experimentally induced diabetic nephropathy in rats.

## AIM OF THE WORK:

This work aimed to evaluate the capability of autologous platelet-rich plasma to alleviate experimentally induced diabetic nephropathy in adult male albino rat.

## MATERIAL AND METHODS:

### Animals:

Forty albino rats were used in this study, rats were adult males, 7-8 months age and 190-200 gm weight. They were kept three /cage with good ventilation (Medical Research Center, Faculty of Medicine, Ain-Shams University), subjected to regular dark/light cycles at room temperature. Food and water were freely allowed except at the fasting periods before induction of diabetes.

Rats were distributed in four groups. each group contained ten rats:

**Group I (control)**: rats were redistributed into two equal subgroups:

- Subgroup a: rats received no treatment for six weeks.
- Subgroup b: each rat was intraperitonially injected by a single dose of citrate buffer (1ml) then kept without any treatment for six weeks.

**Group II (prp):** each rat received prp in a dose 0.5 mL/kg, twice weekly by subcutaneous injection for six weeks.

**Group III (diabetes):** each rat received a single intraperitoneal injection of 55 mg/kg Sz as described below, then after confirmation of diabetes they kept without any treatment for six weeks.

**Group IV (diabetes + prp):** each rat received a single intraperitoneal injection of Sz as in group III and from the day of confirmation of diabetes prp was injected as in group II for six weeks.

### Induction of diabetes:

After overnight food deprivation, each rat received a single intraperitoneal injection of 55 mg/kg Streptozotocin (Sz) (Sigma, St. Louis, Mo, USA), dissolved in 1 ml citrate buffer. Blood samples (tail vein) after three days of injection were taken then the blood glucose level was evaluated (BIONIME GmbH, Switzerland), rats having blood glucose level higher than or equal to 250 mg/dl were included as diabetic rats [12,13]. Rats were then given water containing sucrose (15 gm/Liter) for two days to control early death [14,15].

**Platelet-rich plasma (prp) preparation** (Medical Research Center, Faculty of Medicine, Ain-Shams University)

Two ml of tail vein blood was collected from each rat through a previously dipped capillary tube in 3.2% sodium citrate (Under ether inhalation anesthesia and aseptic condition). The blood was then transferred to tubes with acid citrate dextrose (0.5 mL), then double centrifugation was done (1600 rpm (10 minutes) and 2000 rpm (10 minutes). After centrifugation, the upper part having the platelet-poor plasma was separated, the lower part was kept in the tube and shacked gently to get the platelet suspension (prp). Sample were checked for platelet count by automatic apparatus for >1,000,000/µl. Each rat received subcutaneous injection of 0.5 mL/kg, twice weekly prp diluted in phosphate buffer saline (1:1) through a sterile insulin syringe [16].

**Processing of samples:**

Rats were sacrificed under anesthesia (ether inhalation). The anterior abdominal walls were opened, the kidneys were obtained and washed with saline. The left kidneys were fixed in neutral formalin (10%) then processed for paraffin blocks. While the right kidneys were cut into pieces then fixed in 2.5% glutaraldehyde and processed for epon blocks.

Paraffin blocks were then cut into sections (5µm thickness), sections were stained for histological and immunohisto-chemical examination.

For histological examination Hema-toxylin and Eosin stain (H. & E.) [17] and Mallory trichrome stain "for detection of collagen"[18] were used.

For immunohistochemical staining, caspase3 "apoptosis indicator" was used, sections were incubated with rabbit cleaved caspase3 polyclonal antibody to cleave caspase3 at a dilution of 1:200 (Invitrogen, Sweden AB Stockholm Sweden). The secondary antibody was anti-mouse antibody diluted of 1:500 (Invitrogen, Molecular Probes, Eugene, Oregon, USA) [19].

For semithin sections, 1µm sections from epon blocks were cut by LKB. Ultra-Microtome and stained with toluidine blue.

Ultrathin sections were cut (50 nm) using the ultra-microtome then picked on uncoated copper grids and stained with uranyl acetate and lead citrate [20].

A light microscope with automatic photomicrographic camera (BX3M series, Olympus, Tokyo, Japan) was used at the Anatomy Department (Faculty of Medicine, Ain Shams University) and a transmission electron microscope (Jeol-Ex1010) was used at the regional center of mycology and biotechnology (Al-Azhar University) in examining and photographing the stained sections.

**Morphometric analysis:**

Image-J software (version 1.48v National Institute of Health, Bethesda, Maryland, USA) was used. Ten non overlapping fields of ten dissimilar sections of ten dissimilar rats of each group were used for estimating the mean area % of caspase3, the mean area % of collagen, the mean thickness of the glomerular basement membrane and the mean length of podocyte foot processes in micrometers. The magnification used for estimating caspase3 and collagen was x100 while x12000 was used for the thickness of the glomerular basement membrane and the length of podocyte foot processes. By a stage micrometer, pixels were adjusted for the actual measurements.

**Statistical analysis:**

SPSS software (version 20, IBM Corp., Armonk, NY, USA), one-way ANOVA and Bonferroni Post Hoc test were used. Differences between rats' groups (I, III and IV) were compared. Data (mean value ± standard deviation and p-value) presented in tables and histograms. P-value was considered highly significant if ≤ 0.001, significant if ≤ 0.05 and non-significant if > 0.05.

**Ethical Consideration:**

The Research Ethics Committee approved this experiment with the approval No. FMSAU R147/2023, Faculty of Medicine, Ain Shams University.

## RESULTS:

**Examination of H.&E.-stained sections and toluidine blue stained semithin sections.**

Group I (a &b) and group II showed the same regular structure of the renal cortex; several regular renal tubules (proximal and distal convoluted tubules) and renal corpuscles. The proximal tubules were numerous, lined by cubical cells with basal vesicular nuclei and they were having narrow lumina. While the distal tubules were less numerous, lined by cubical cells with apical or central vesicular nuclei and having wide lumina**.** The simple squamous epithelium of the parietal layer of Bowman's capsule was surrounding the renal corpuscle, while the visceral layer of the capsule was lined by the podocytes. A regular Bowman's space between the two layers was noticed.

The renal glomeruli appeared occupying most of the renal corpuscles, they were formed of glomerular capillaries, deeply stained intra-glomerular mesangial cells and podocytes with pale stained cytoplasm and nuclei. Small interstitial blood vessels were also noticed (Figs. 1-3).

Group III, the renal tubules showed cytoplasmic vacuolations with hardly identified nuclei in their lining cells. The renal corpuscles had hypertrophied glomeruli, obliterated Bowman's space, dark stained podocytes, enlarged mesangial cells and collapsed lumina of some capillaries. Dilated congested interstitial blood vessels with interstitial hemorrhage were also noticed (Figs. 4&5).

Group IV showed almost intact proximal and distal renal tubules, regular renal corpuscles and small interstitial blood vessels (Figs. 6&7).

**Examination of sections stained with Mallory trichrome.**

Group I (a &b) and group II showed scanty collagen fibers around the renal tubules and in the two layers of Bowman's capsule (Fig. 8).

Group III showed dense collagen fibers around the renal tubules and in the two layers of Bowman's capsule (Fig. 9).

Group IV showed mild to moderate amount of collagen fibers around the renal tubules and in the two layers of Bowman's capsule (Fig. 10).

**Examination of ultrathin sections.**

Group I (a &b) and group II showed the cells of the renal tubules having regular euchromatic nuclei, apical microvilli (numerous in proximal tubules), basal numerous longitudinal mitochondria and thin regular basement membrane (Fig. 11).

Group III showed the cells of the renal tubules with irregular nuclei compressed by cytoplasmic vacuolations, cytoplasmic lysosomes, scanty apical microvilli, scanty basal mitochondria and thick basement membrane (Fig. 12).

Group IV showed intact ultrastructure of the cells of the renal tubules; regular euchromatic nuclei, apical microvilli (numerous in proximal tubules), basal numerous longitudinal mitochondria and regular basement membrane (Fig. 13).

Additionally, both groups showed renal glomerular filtration barrier consisted of glomerular basement membrane "with regular thickness" between narrow fenestrated capillary endothelium and long podocyte foot processes "interconnected with slit diaphragm" (Figs. 14,15).

Group III showed renal glomerular filtration barrier having irregular thick glomerular basement membrane, interrupted

capillary endothelium with wide fenestrations and short podocyte foot processes with interrupted interconnecting slit diaphragm (Fig. 16).

Group IV showed renal glomerular filtration barrier having slightly irregular glomerular basement membrane between relatively narrow fenestrated capillary endothelium and long podocyte foot processes with intact interconnecting slit diaphragm (Fig. 17).

**Examination of sections immunohistochemically stained with caspase 3.**

Group I (a &b) and group II showed negative immune reaction of the cells inside the renal corpuscles and the cells of the renal tubules (Fig. 18).

Group III showed strong positive immune reaction of the cells inside the renal corpuscles and the cells of the renal tubules (Fig. 19).

Group IV showed negative immune reaction of the cells inside the renal corpuscles and weak positive reaction of the cells of the renal tubules (Fig. 20).

**Morphometric results and statistical analysis:**

Morphometric measures and statistical analysis of the groups I, III and IV revealed high significant difference between group I and III and between group III and IV for the mean area % of collagen, the mean area % of caspase3, the mean thickness of the glomerular basement membrane and the mean length of the podocyte foot processes and non-significant difference between group I and IV regarding the mean area % of caspase 3, the mean thickness of glomerular basement membrane and the mean length of podocyte foot processes with a significate difference between group I and IV regarding the mean area % of collagen. Data were displayed in tables and histograms.

**Table (1):** displaying the mean area % of caspase 3 and the mean area % of collagen. P-value highly significant (*), significant (**) and nonsignificant (***).

| | **Area % of caspase 3** | **Area% of collagen** |
|---|---|---|
| **Mean ± Standard deviation** | | |
| **Group I** | 0.37± 0.03 | 3.28±0.07 |
| **Group III** | 47.1 ± 1.09 | 13.99± 1.1 |
| **Group IV** | 0.6± 0.19 | 3.77± 0.3 |
| **P-value** | | |
| **Groups I & III** | 0.00001 | 0.00001* |
| **Groups I & IV** | 0.1*** | 0.01** |
| **Groups III & IV** | 0.00001* | 0.00001* |

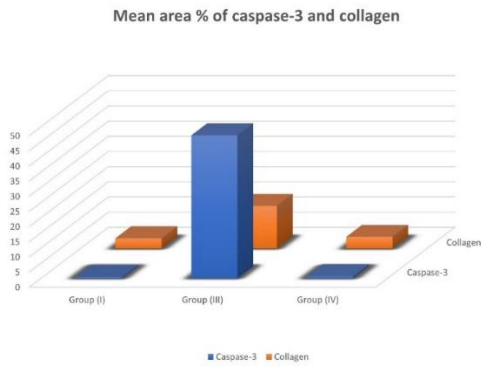


**Histogram (1):** displaying the mean area % of caspase 3 and mean area % of collagen.

**Table (2):** displaying the mean thickness of glomerular basement membrane and the mean length of podocyte foot processes in µm. P-value highly significant (*), significant (**) and nonsignificant (***).

| | Glomerular basement membrane | Podocyte foot processes |
|---|---|---|
| Mean ± Standard deviation | | |
| Group I | 24.04± 0.61 | 161±0.66 |
| Group III | 67.1 ± 0.12 | 103± 0.64 |
| Group IV | 25.2± 0.62 | 159.9± 0.32 |
| P-value | | |
| Groups I& III | 0.00001* | 0.00001* |
| Groups I& IV | 0.08*** | 0.3*** |
| Groups III & IV | 0.00001* | 0.00001* |

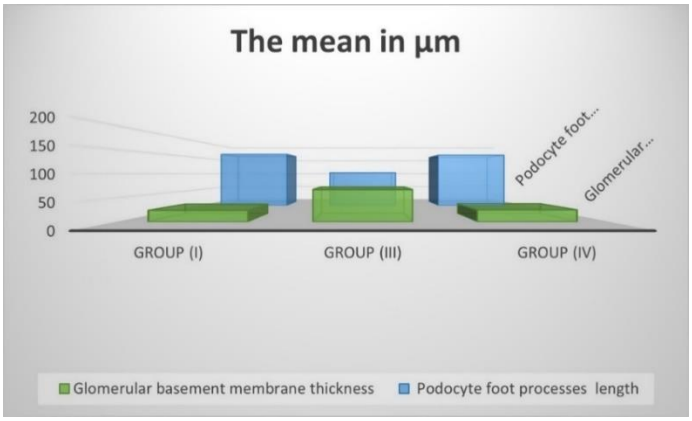


**Histogram (2):** displaying the mean thickness of glomerular basement membrane and the mean length of podocyte foot processes in µm.

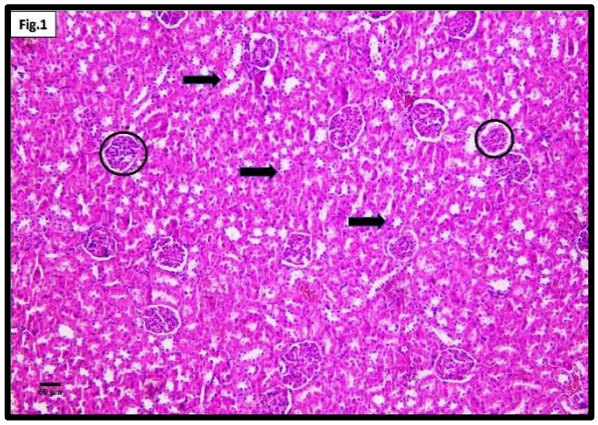


**Fig. 1:** A photomicrograph of a rat's renal cortex from group (I) showing multiple regular renal corpuscles (circles) and multiple regular renal tubules (black arrows). (H.&E., x100)

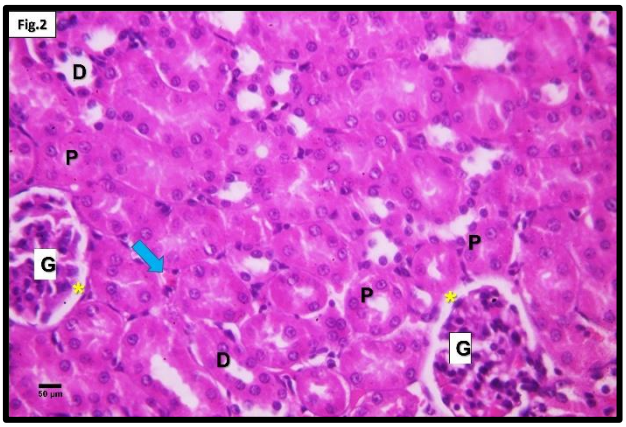


**Fig. 2**: A photomicrograph of a rat's renal cortex from group (I) showing regular renal corpuscles occupied mostly by their glomeruli (G), regular Bowman's spaces (*), numerous proximal tubules with narrow lumina (P) and less numerous distal tubules with wide lumina (D). Notice the small interstitial blood vessel (blue arrow). (H.&E., x400)

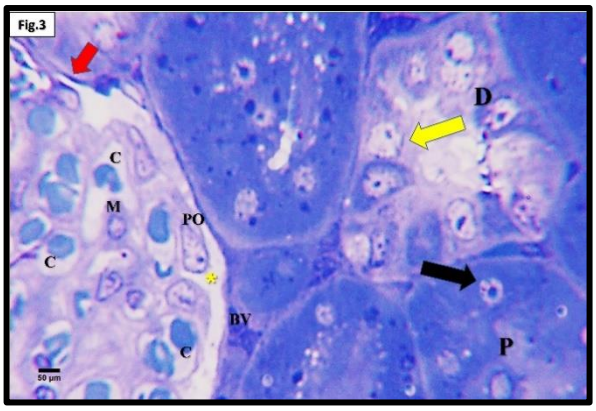


**Fig. 3**: A photomicrograph of a semithin section of a rat's renal cortex from group (I) showing the proximal tubules (P) lined by cubical cells with basal vesicular nuclei (black arrows), the distal tubules (D) lined by cubical cells with central vesicular nuclei (yellow arrows), a part of renal corpuscle with its glomerulus surrounded by the parietal layer of Bowman's capsule (red arrow), podocyte (PO) with pale cytoplasm and pale nucleus and Bowman's space (*). Notice, the glomerular capillaries (C), the deeply stained intra-glomerular mesangial cells (M) and the small interstitial blood vessel (BV).
(Toluidine blue, x1000)

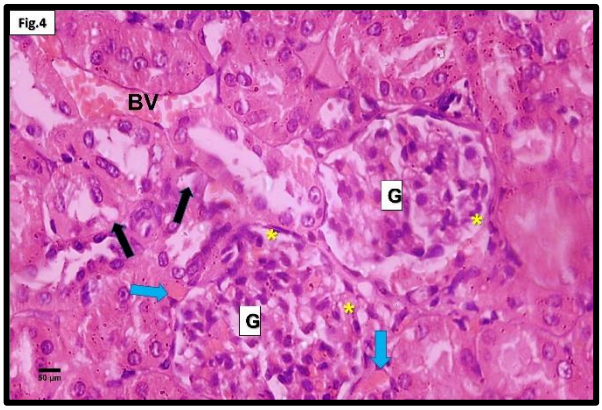


**Fig. 4**: A photomicrograph of a rat's renal cortex from group (III) showing renal corpuscles with hypertrophied glomeruli (G), irregular narrow Bowman's space (*), vacuolated lining cells of the renal tubules (black arrows). Notice, the dilated congested interstitial blood vessels (BV) with interstitial hemorrhage (blue arrows). (H.&E. x400)

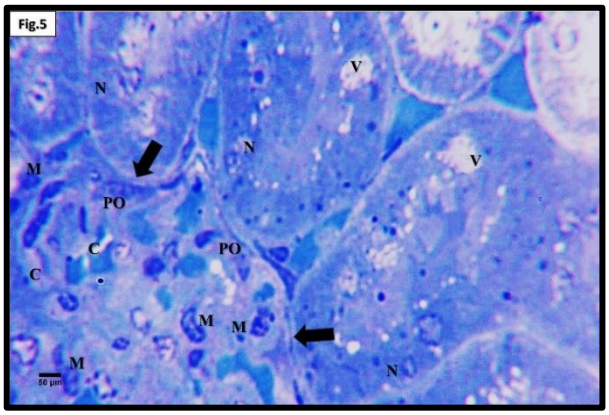


**Fig. 5:** A photomicrograph of a semithin section of a rat's renal cortex from group (III) showing the cells of the renal tubule mostly with hardly identified nuclei (N) and multiple cytoplasmic vacuoles (V), a part of renal corpuscle having nearly obliterated Bowman's space (black arrows), dark stained podocytes (PO), enlarged mesangial cells (M) and collapsed some capillaries lumina (C).
(Toluidine blue, x1000)

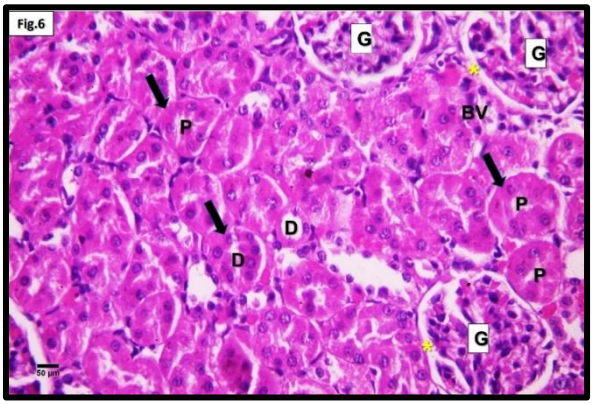


**Fig. 6**: A photomicrograph of a rat's renal cortex from group (IV) showing regular renal corpuscles occupied mostly by their glomeruli (G), regular Bowman's spaces (*), intact cuboid cells (black arrows) lining the proximal (P) and distal (D) renal tubules. Notice, the small interstitial blood vessels (BV). (H.&E., x400)

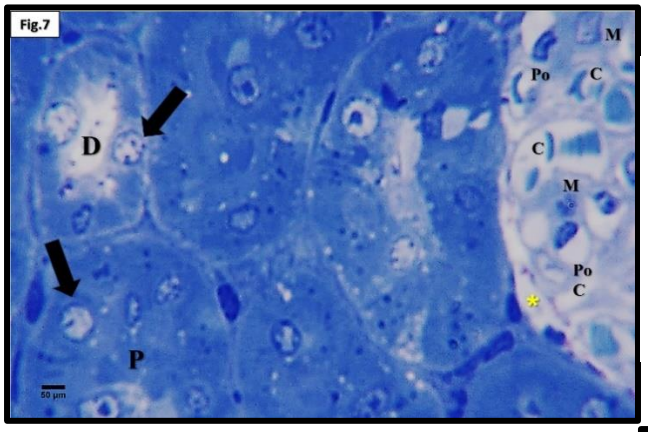


**Fig. 7**: A photomicrograph of a semithin section of a rat's renal cortex from group (IV) showing the renal tubules, proximal (P) and distal (D) lined by cubical cells with vesicular nuclei (black arrows), a part of renal corpuscle with podocyte (PO) having pale stained cytoplasm and nucleus, small mesangial cells (M). Notice, the glomerular capillaries (C) and the Bowman's space (*).
(Toluidine blue, x1000)

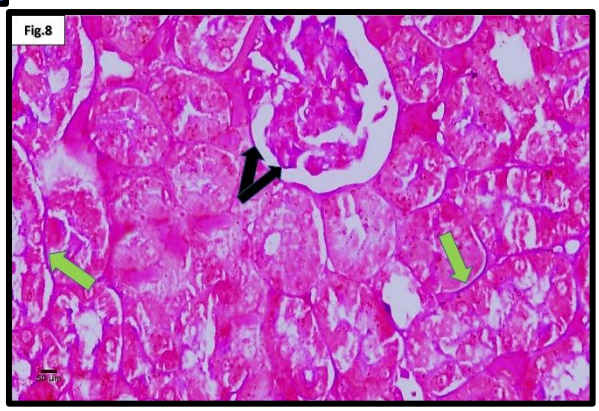


**Fig. 8**: A photomicrograph of a rat's renal cortex from group (I) showing scanty collagen fibers (blue color) around the renal tubules (green arrows) and in the two layers of Bowman's capsule (black arrows). (Mallory trichrome, x400)

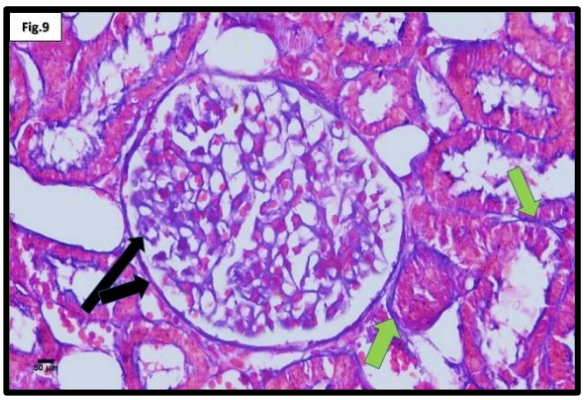


**Fig. 9**: A photomicrograph of a rat's renal cortex from group (III) showing dense collagen fibers (blue color) around the renal tubules (green arrows) and in the two layers of Bowman's capsule (black arrows). (Mallory trichrome, x400)

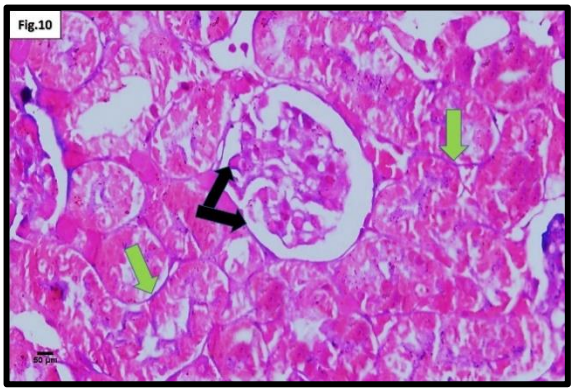


**Fig. 10**: A photomicrograph of a rat's renal cortex from group (IV) showing mild to moderate amount of collagen fibers around the renal tubules (green arrows) and in the two layers of Bowman's capsule (black arrows). (Mallory trichrome x400)

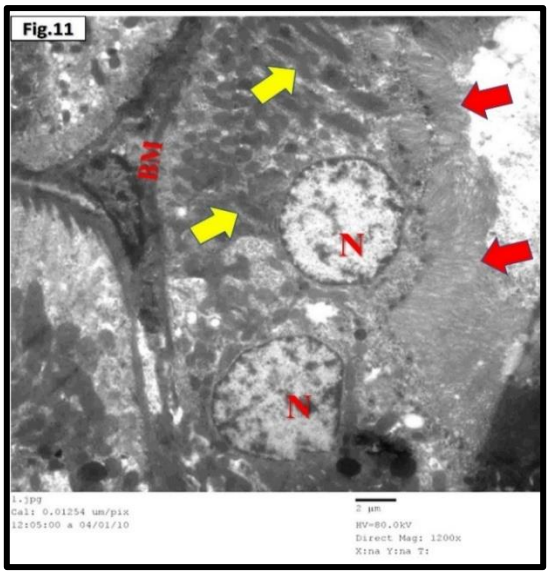


**Fig. 11**: A transmission electron photomicrograph from group (I) showing a part of a renal tubule's (proximal) lining cells with regular euchromatic nuclei (N), numerous apical microvilli (red arrows), basal numerous longitudinal mitochondria (yellow arrows) and thin regular basement membrane (BM). (Uranyl Acetate & Lead Citrate, x1200)

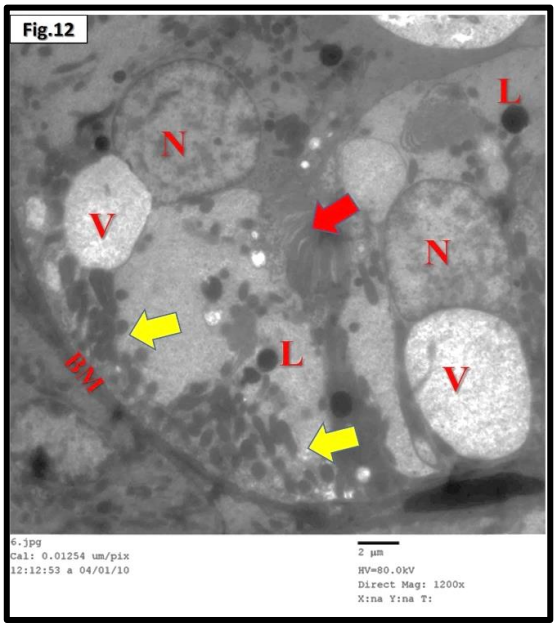


**Fig. 12:** A transmission electron photomicrograph from group (III) showing a part of a renal tubule's (proximal) lining cells with irregular nuclei (N), cytoplasmic vacuolations (V), cytoplasmic lysosomes (L), scanty apical microvilli (red arrow), scanty basal mitochondria (yellow arrows) and thick basement membrane. (Uranyl Acetate & Lead Citrate, x1200)

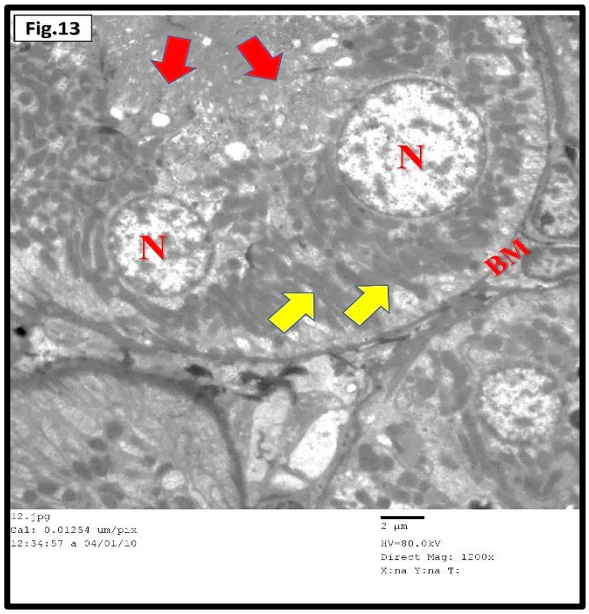


**Fig. 13:** A transmission electron photomicrograph from group (IV) showing a part of a renal tubule's (proximal) lining cells with regular euchromatic nuclei (N), numerous apical microvilli (red arrows), basal numerous longitudinal mitochondria (yellow arrows) and thin regular basement membrane (BM). (Uranyl Acetate & Lead Citrate, x1200)

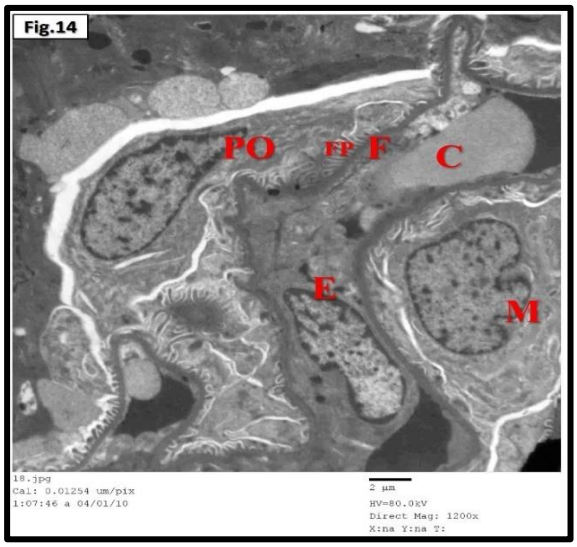


**Fig. 14**: A transmission electron photomicrograph from group (I) showing a part of renal glomerulus with podocyte (PO) foot processes (FP), filtration barrier (F) and endothelial cell (E) lining the capillary lumen (C). Notice the mesangial cells (M). (Uranyl Acetate & Lead Citrate, x1200)

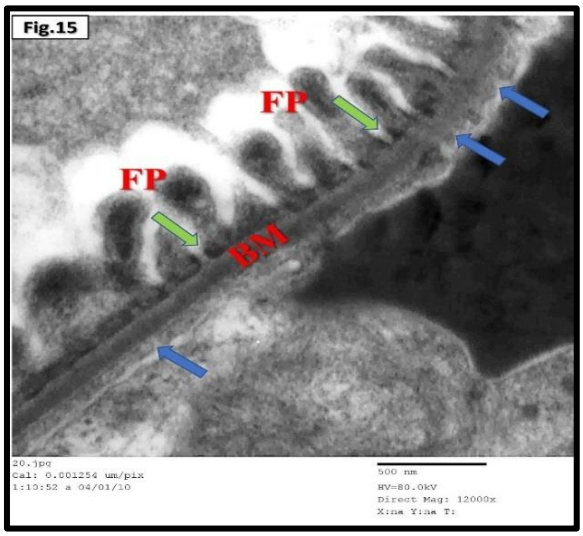


**Fig. 15:** A transmission electron photomicrograph from group (I) showing a part of renal glomerulus' filtration barrier with regular basement membrane (BM) between narrow fenestrated capillary endothelium (blue arrows) and long podocyte foot processes (FP) interconnected with slit diaphragm (green arrows). (Uranyl Acetate & Lead Citrate x12000)

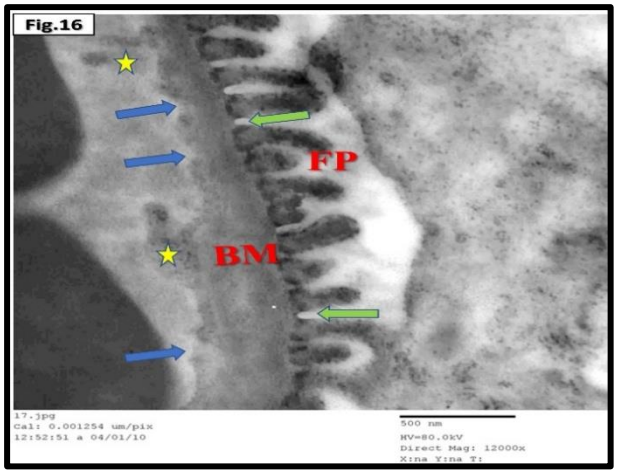


**Fig. 16**: A transmission electron photomicrograph from group (III) showing a part of renal glomerulus' filtration barrier with irregularly thickened basement membrane (BM), interrupted capillary endothelium (*) with wide fenestration (blue arrows) and short podocyte foot processes (FP) with interrupted interconnecting slit diaphragm (green arrows). (Uranyl Acetate & Lead Citrate, x12000)

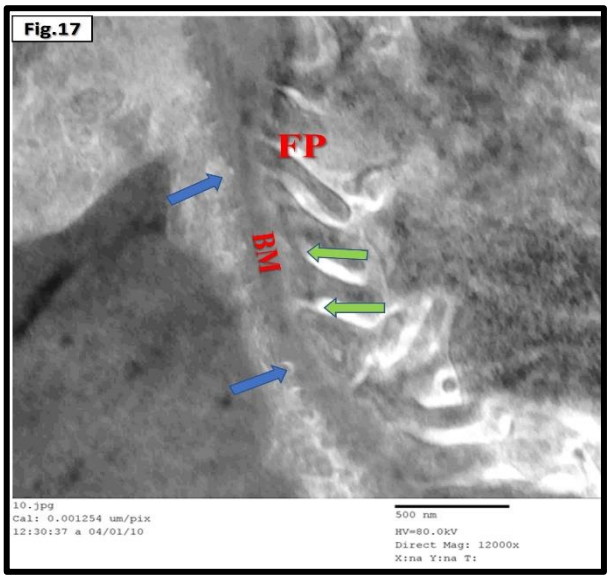


**Fig. 17:** A transmission electron photomicrograph from group (IV) showing a part of renal glomerulus' filtration barrier with slightly irregular basement membrane (BM), relatively narrow fenestrated capillary endothelium (blue arrows) and long podocyte foot processes (FP) with intact interconnecting slit diaphragm (green arrows). (Uranyl Acetate & Lead Citrate, x12000)

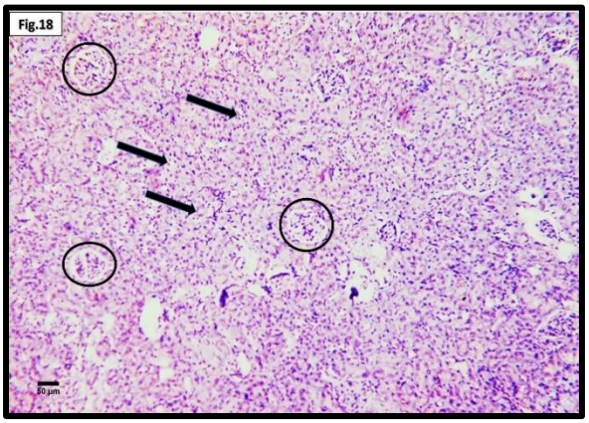


**Fig. 18:** A photomicrograph of a rat's renal cortex from group (I) showing negative immune reaction of the cells inside the renal corpuscles (circles) and the cells of the renal tubules (black arrows). (Caspase3, x100)

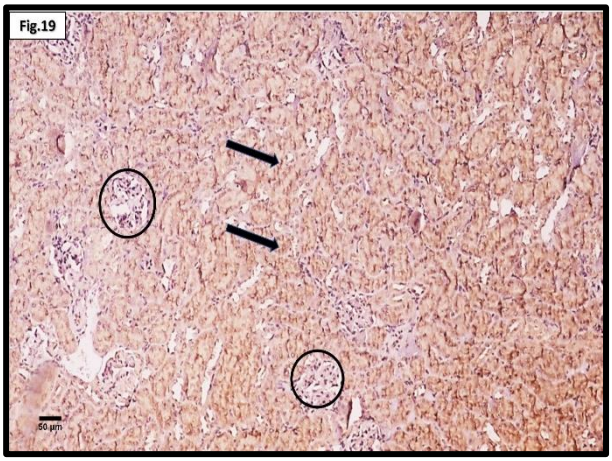


**Fig. 19:** A photomicrograph of a rat's renal cortex from group (III) showing strong positive immune reaction (brown color) of the cells inside the renal corpuscles (circles) and the cells of the renal tubules (black arrows). (Caspase3, x100).

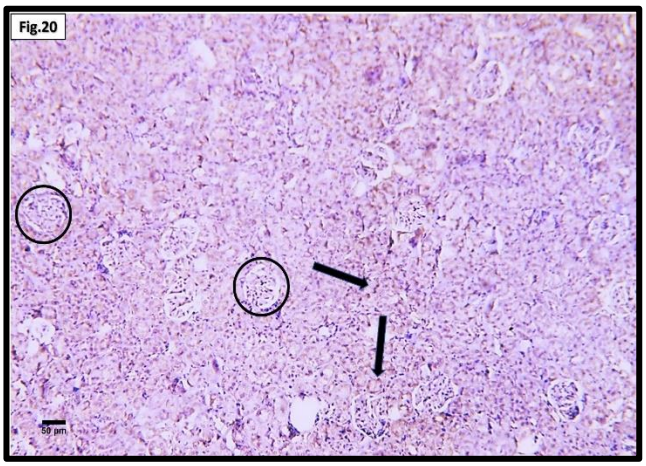


**Fig. 20**: A photomicrograph of a rat's renal cortex from group (IV) showing negative immune reaction of the cells inside the renal corpuscles (circles) and weak positive reaction of the cells of the renal tubules (black arrows). (Caspase3, x100).

## DISCUSSION:

Diabetes mellitus has become one of the world's most important health problems. Number of diabetic patients is anticipated to reach 592 million worldwide in 2035 (according to the International Diabetes Federation). Diabetic nephropathy is a common complication of diabetes [(21)]. Multiple mechanisms were described as the underlying causes of diabetic nephropathy, including increased production of reactive oxygen species and type IV collagen, inflammation, hemodynamic changes [(4)] and DNA methylation; where the methyl group of S-adenosylmethionine is transported to the cytosine of the DNA that activates the immune response [(22)].

In the current study, the capability of autologous platelet rich plasma to alleviate experimentally induced diabetic nephropathy in rats was evaluated histologically and confirmed by the morphometric study and the statistical analysis.

Six weeks duration after induction of diabetes was chosen to assess the development of diabetic nephropathy, as the changes of diabetic nephropathy started to develop after three weeks from Sz injection in rats **(15).**

Diabetic rats that received no treatment showed renal corpuscles with hypertrophied glomeruli, mesangial expansion, obliterated Bowman's space, some collapsed capillaries and degenerated podocytes. Also, the glomerular filtration barrier showed thick irregular glomerular basement membrane, interrupted capillary endothelium with wide fenestration and short podocyte foot processes with interrupted slit diaphragm. The statistical analysis revealed high significant difference between the control group and the diabetic group regarding the glomerular basement membrane thickness and the podocyte foot processes length.

Similar changes in the structure of the renal glomeruli with degenerative changes in the renal tubules were reported by Ebrahim et al. **(23)** and El-Sokkary et al.**(24)** in untreated diabetic rats.

Podocytes' role in the renal glomeruli is keeping up the glomerular basement membrane selectivity. The slit diaphragm is a very specialized intercellular junction between podocyte foot processes that is pivotal in the formation of the filtration barrier. Losing the integrity of podocytes' slit diaphragm leads to disturbance of the filtration barrier and subsequently excretion of protein in urine (proteinuria). Nephrin and Podocin proteins are integral proteins of the slit diaphragms which are essential for the construction of the filtration barrier. Defective production of these proteins occurs in diabetic nephropathy leading to abnormal thickening of glomerular basement membrane and alteration of the filtration process **(25-26)**.

Mesangial expansion is used in the diagnosis of diabetic nephropathy and is marked by aberrant proliferation of mesangial cells **(27).** By the effect of increased production of free oxygen radicals and high glucose level that occur with diabetes, the extracellular matrix proteins produced by the mesangial cells increase in addition to abnormal glycosylation of mesangial matrix proteins which interfere with their turnover, subsequently leading to mesangial expansion and thickening of glomerular basement membrane **(28)**. Mesangial expansion occludes the glomerular capillaries **(29).**

Moreover, in the current study the renal tubules of the diabetic rats showed degenerated cells with cytoplasmic vacuoles and lysosomes, scanty apical microvilli, scanty basal mitochondria and thick basement membrane. In addition to congested interstitial blood vessels with interstitial hemorrhage, increased cellular apoptosis and increased collagen deposition. The statistical analysis revealed high significant difference between the control group and the diabetic group regarding collagen content and apoptosis.

Tubular cells vacuolization could be attributed to the deposition of glycogen and lipid in cytoplasmic vacuoles which commonly occur with diabetic nephropathy **(30)**. The proximal convoluted tubules are richer in mitochondria and apical microvilli than the distal tubules. They absorb most of the electrolytes and almost completely the glucose and the amino acids filtered by the glomeruli. Prolonged hyperglycemia leads to glycogen accumulation in renal tubules which indicates abnormal reabsorption of glucose or disturbed transporting the reabsorbed glucose to the blood capillaries. Mitochondrial dysfunction in renal tubular cells which occurs with diabetes due to

increased production of reactive oxygen species leads to cellular apoptosis [31&32].

Increase collagen, laminin, and fibronectin deposition are well known causes of increased glomerular basement membrane thickness, tubular damage and increased extracellular matrix in diabetic nephropathy [33]. Increase collagen production in diabetic kidney is associated with exposure to increased oxidative stress [34]. The different cell types of the kidney can be destroyed by diabetes, any damage of one cell type affects the other types of cells [35].

In the current study, platelet-rich plasma alleviated the development of diabetic nephropathy changes; the renal corpuscles were almost having regular structure, the filtration barrier of the renal glomeruli showed slightly irregular glomerular basement membrane with long podocyte foot processes and intact slit diaphragm. The renal tubules were intact with apical microvilli, basal longitudinal mitochondria and regular basement membrane. In addition to non-congested interstitial blood vessels. However, minimal apoptosis in renal tubular cells and mild to moderate increase in collagen deposition were still detected.

The statistical analysis revealed nonsignificant difference between the control group and diabetic group that received prp, regarding apoptosis, glomerular basement membrane thickness and podocyte foot processes length, a significate difference between the same groups regarding the collagen content and a high significant difference between the diabetic group and the diabetic group that received prp for the four measures.

In a prior study on diabetic rats, platelet-rich plasma induced neo-vascularization and restored pancreatic islet cells which subsequent led to lowering the blood glucose level [36]. It has been proved that platelet-rich plasma also able to activate phosphatidylinositol-3 kinase pathway that reduces free radicals' production and antagonize the oxidative stress [37].

Platelet-rich plasma has anti-apoptotic, anti-fibrotic and anti-inflammatory effects on many organs such as kidneys, lungs, peripheral nerves and liver. Its anti-inflammatory effect is attributed to its high content of growth factors and chemokine ligand-5 which inhibit cytokines release and raise the level of anti-inflammatory lipoxin A4[37-40].

Regarding its anti-apoptotic effect, it reduces the expression of kinase-1signal that modulates protein 3 kinase that eventually modulates the pathways of cellular proliferation and programmed cell death [41]. Also, platelet-rich plasma able to decrease caspase3 activity which was reported when tested on testicular tissue ischemia/reperfusion injury in a rat model [42].

Platelet-rich plasma can attenuate the progression of fibrosis in different tissues by decreasing collagen deposition. In a prior study on damaged endometrium of female rats, platelet-rich plasma attenuated excessive deposition of collagen in the endometrium [43]. Additionally, in the current study it attenuated excessive collagen deposition in diabetic kidneys.

### Conclusion

Autologous platelet rich plasma could alleviate the histological changes of diabetic nephropathy in adult male albino rats.

## Conflict of Interest:

No conflict of interest

### REFERENCES

1. **Rico-Fontalvo J, Aroca G, Cabrales J, Daza-Arnedo R, Yánez-Rodríguez T, Martínez-Ávila MC et al**. Molecular Mechanisms of Diabetic Kidney Disease. International Journal of Molecular Sciences. 2022;23(15):2-16.

2. **Delrue C, Speeckaert R, Delanghe JR and Speeckaert MM.** The Role of vitamin D in diabetic nephropathy: A translational approach. Int. J. Mol. Sci. 2022; 23:2-17.

3. **Thomas MC, Brownlee M, Susztak K, Sharma K, Jandeleit-Dahm KA, Zoungas S, Rossing P et al.** Diabetic kidney disease. Nat Rev Dis Primers. 2015; 30(1): 1-46.

4. **Tuttle KR, Agarwal RL, Alpers CE, Bakris GL, Brosius FC, Kolkhof P et al**. Molecular mechanisms and therapeutic targets for diabetic kidney disease. Kidney International. 2022;102(2):248-260.

5. **Turgut F and Bolton WK**. Potential new therapeutic agents for diabetic kidney disease. Am J Kidney Dis. 2010;55(5):928-940.

6. **Roohaninasab M, Goodarzi A, Ghassemi M, Sadeghzadeh-Bazargan A, Behrangi E and Nobari NN.** Systematic review of platelet-rich plasma (PRP) in treating alopecia: focusing on efficacy, safety, and therapeutic durability. Dermatol Ther. 2021;34(2): 1-9.

7. **Luzo A, Fávaro W, Seabra A and Duran N.** What is the potential use of platelet-rich-plasma (PRP) in cancer treatment? A mini review. Heliyon, 2020; 6 (3): 1-9.

8. **Murata S, Ohkohchi N, Matsu R, Ikeda O, Myronovych A and Hoshi R**. Platelets promote liver regeneration in early period after hepatectomy in mice. World Journal of Surgery. 2007; 31(4): 808-816.

9. **Hafez SMNA, Zenhom NM and Abdel-Hamid HA**. Effects of platelet rich plasma on experimentally induced diabetic heart injury. International Immunopharmacology. 2021; 96: 107814.

10. **Ismail DI and Farag EA**. Histological Study on Platelet Poor Plasma versus Platelet Rich Plasma in Amelioration of Induced Diabetic Neuropathy in Rats and the Potential Role of Telocyte-like Cells. 2021;44(1):8-30.

11. **Ahmed SF, Saif-Elnasr M, and Fattah SMA.** Platelet-rich plasma ameliorates gamma radiation-induced nephrotoxicity via modulating oxidative stress and apoptosis." Life sciences.2019; 219: 238-247.

12. **Hünkar T, Aktan F, Ceylan A and Karasu C.** Antioxidants in Diabetes-Induced Complications (ADIC) Study Group. Effects of cod liver oil on tissue antioxidant pathways in normal and streptozotocin-diabetic rats. Cell Biochem Funct. 2002;20(4): 297-302.

13. **Akbarzadeh A, Norouzian D, Mehrabi MR, Jamshidi SH, Farhangi A, Verdi AA et al.** Induction of diabetes by Streptozotocin in rats. Indian J Clin Biochem. 2007; 22 (2):60-64.

14. **Davis BJ, Johnston CI, Burrell LM, Burns WC, Kubota E, Cao Z et al.** Renoprotective effects of vasopeptidase inhibition in an experimental model of diabetic nephropathy. Diabetologia. 2003; 46(7):961-971.

15. **Tesch GH and Allen TJ.** Methods in Renal Research: Rodent models of streptozotocin-induced diabetic nephropathy. Nephrology. 2007; 12: 261–266.

16. **El-Tahawy N, Rifaai R, Saber E, Saied S and Ibrahim A**. Effect of platelet rich plasma (prp) injection on the endocrine pancreas of the experimentally induced diabetes in male albino rats: A histological and immunohistochemical study. J Diabetes Metab. 2017; 8(730):2-5.

17. **Kiernan JA**. Histological and Histochemical Methods: Theory and Practice 5th edition, Scion Publishing Ltd, Banbury, UK. 2015, pp 571.

18. **Ross M and Oawlina W. Histology**: A Text and Atlas (6th Ed.). Lippincott Williams & Wilkins. 2011, pp 5–6.

19. **Stenberg L, Kanje M, Dolezal K and Dahlin LB**. Expression of activating transcription factor 3 (ATF 3) and caspase 3 in Schwann cells and axonal outgrowth after sciatic nerve repair in diabetic BB rats. Neuroscience letters. 2012; 515 (1): 34-38.

20. **Reynolds ES**. The use of lead citrate of high pH as an electron opaque stain in electron microscopy. J cell Biol. 1963; 17: 208-240.

21. **Shi Y and Hu FB**. The global implications of diabetes and cancer. Lancet 383, 2014, pp1947–1948.
22. **Shao BY, Zhang, SF, Li HD, Meng XM and Chen HY**. Epigenetics and Inflammation in Diabetic Nephropathy. Front. Physiol. 2021; 12:1-14.
23. **Ebrahim R, Mostafa O and Mohamed E**. Effect of Low and High Doses of Vitamin D on Streptozotocin Induced Diabetic Nephropathy in Adult Male Albino Rats: Histological and Immunohistochemical Study. EJH. 2019; 42(3):699-711.
24. **El-Sokkary NH, Yusuf A, Abdel-Moneim RA, Abdulrazeg HS and Hassaan PS**. The possible ameliorative effect of vitamin D3 and/or omega-3 fatty acids in a rat model of type I early diabetic nephropathy: A physiological and histological study Bull. Egypt. Soc. Physiol. Sci. 2021; 42(1):101-117.
25. **Martin CE and Jones N**. Nephrin Signaling in the Podocyte: An Updated View of Signal Regulation at the Slit Diaphragm and Beyond. Front Endocrinol. 2018; 9:1-12.
26. **El-Sokkary NH, Yusuf A, Abdel-Moneim RA, Abdulrazeg HS, Passainte S. Hassaan.** The possible ameliorative effect of vitamin D3 and/or omega 3 fatty acids in a rat model of type I early diabetic nephropathy: A physiological and histological study. Bull. Egypt. Soc. Physiol. Sci. 2021;42(1): 101-117.
27. **Thomas HY and Ford Versypt AN.** Pathophysiology of mesangial expansion in diabetic nephropathy: mesangial structure, glomerular biomechanics, and biochemical signaling and regulation. J Biol Eng. 2022;16 (19):1-13.
28. **Ha H and Lee HB**. Reactive oxygen species and matrix remodeling in diabetic kidney. J Am Soc Nephrol. 2003; 14:246-249.
29. **Abrass CK**. Diabetic nephropathy: Mechanisms of mesangial matrix expansion. West J Med. 1995;162(4):318-321.
30. **Pourghasem M, Shafi H and Babazadeh Z.** Histological changes of kidney in diabetic nephropathy. Caspian journal of internal medicine. 2015; 6 (3):120-127.
31. **Lei P, Bai T and Sun Y**. Mechanisms of Ferroptosis and Relations with Regulated Cell Death: A Review, Front. Physiol.2019; 10 (139):1-13.
32. **Chang J, Yan J, Li X, Liu N, Zheng R and Zhong Y.** Update on the Mechanisms of Tubular Cell Injury in Diabetic Kidney Disease. Front Med. 2021; 8:1-12.
33. **Najafian B, Alpers CE and Fogo AB**. Pathology of human diabetic nephropathy. In Diabetes and the Kidney. 2011; 170:36-47.
34. **Szostak J, Gorący A, Durys D, Dec P, Modrzejewski A and Pawlik A**. The Role of MicroRNA in the Pathogenesis of Diabetic Nephropathy. International Journal of Molecular Sciences. 2023; 24(7):1-15.
35. **Maezawa Y, Takemoto M and Yokote K.** Cell biology of diabetic nephropathy: Roles of endothelial cells, tubulointerstitial cells and podocytes. Journal of diabetes investigation. 2015; 6 (1): 3-15.
36. **El-Tahawy NF, Rifaai RA, Saber EA, Saied SR and Ibrahim RA.** Effect of platelet rich plasma (prp) injection on the endocrine pancreas of the experimentally induced diabetes in male albino rats: a histological and immunohistochemical study. J Diabetes Metab. 2017; 8: 730-739.
37. **Tong S, Zhang C and Liu J.** Platelet-rich plasma exhibits beneficial effects for rheumatoid arthritis mice by suppressing inflammatory factors". Molecular Medicine Reports. 2017:16: 4082-4088.
38. **Zhang J, Middleton KK, Fu FH, Im HJ and Wang JH.** HGF mediates the anti-inflammatory effects of PRP on injured tendons. PLoS One. 2013; 8(6):1-12.
39. **Abdul Ameer LA, Raheem ZJ, Abdulrazaq SS, Ali BG, Nasser MM, Khairi AWA.** The anti-inflammatory effect of the platelet-rich plasma in the periodontal pocket. Eur J Dent.2018; 12: 528–531.
40. **Alves R and Grimalt R.** A Review of Platelet-Rich Plasma: History, Biology,

Mechanism of Action, and Classification. Skin Appendage Disorders. 2018; 4:18–24.

41. **Martini L, Via AG, Fossati C, Randelli F, Randelli P and Cucchi D**. Single Platelet-Rich Plasma Injection for Early Stage of Osteoarthritis of the Knee. Joints. 2017; 5 (1):2-6.

42. **Sekerci CA, Tanidir Y, Sener TE, Sener G, Cevik O, Yarat A et al**. Effects of platelet-rich plasma against experimental ischemia/reperfusion injury in rat testis J. Pediatr. Urol. 2017; 13 (3): 1-9.

43. **Jang HY, Myoung SM, Choe JM, Kim T, Cheon YP, Kim YM et al**. Effects of Autologous Platelet-Rich Plasma on Regeneration of Damaged Endometrium in Female Rats. Yonsei Medical Journal. 2017; 58 (6):1195-1203.

# قدرة البلازما الذاتية الغنية بالصفائح الدموية على التخفيف من إعتلال الكلى السكري المستحث تجريبياً على ذكر الفأر الأبيض البالغ (دراسة بالمجهر الضوئى والإلكترونى)

**إيناس أنور بخيت**

قسم التشريح والأجنة - كلية الطب - جامعة عين شمس

**مقدمة:** يعد اعتلال الكلى السكري هو أحد المضاعفات الشائعة لمرض السكري. في دراسات السابقة ، خففت البلازما الغنية بالصفائح الدموية من إصابة القلب السكري واعتلال الأعصاب السكري.

**الهدف:** يهدف هذا العمل إلى تقييم قدرة البلازما الذاتية الغنية بالصفائح الدموية على التخفيف من اعتلال الكلي السكري المستحث تجريبياً في ذكور الفئران البيضاء.

**المواد والطرق:** تم استخدام أربعين فأرمن الذكور البالغة فى هذه الدراسة. تم توزيع الفئران في أربع مجموعات متساوية:

المجموعة الأولى (المجموعة الضابطة): تم تقسيمها إلى مجموعتين فرعيتين متساويتين:

-المجموعة الفرعية أ: لم تتلق الفئران أي علاج لمدة ستة أسابيع.

-المجموعة الفرعية ب: تم حقن كل فأر داخل الصفاق بجرعة واحدة من محلول السترات (1 مل) ثم احتفظ بها دون أي علاج لمدة ستة أسابيع.

-المجموعة الثانية (مجموعة البلازما الغنية بالصفائح الدموية): تلقى كل فأر 0.5 مل / كجم من البلازما الغنية بالصفائح الدموية ، مرتين أسبوعياً عن طريق الحقن تحت الجلد لمدة ستة أسابيع.

المجموعة الثالثة (مجموعة السكري): تلقى كل فأر 55 مجم / كجم من الستربتوزوتوسين ، حقنة واحدة داخل الصفاق ، ثم احتفظ بها دون أي علاج لمدة ستة أسابيع .

-المجموعة الرابعة ( السكري + البلازما الغنية بالصفائح الدموية) تلقى كل فأر حقنة واحدة داخل الصفاق من الستربتوزوتوسين كما في المجموعة الثالثة ومن يوم تأكيد الإصابة بمرض السكري تم حقن مجموعة البلازما الغنية بالصفائح الدموية كما في المجموعة الثانية.

**النتائج:** أظهرت المجموعة المصابة بالسكري أن خلايا الأنابيب الكلوية تحتوي على فجوات سيتوبلازمية مع قلة فى الزغيبات القمية والميتوكوندريا القاعدية. و فى الوقت نفسه أظهرت الكريات الكلوية تضخم الكبيبات، وتضخم خلايا المسراق الكبيبة. بينما اظهرت المجموعة التى تلقت البلازما الغنية بالصفائح الدموية بعد الاصابة بالسكري وجود أنابيب كلوية وكريات كلوية سليمة تقريبًا.

**الاستنتاج:** يمكن للبلازما الذاتية الغنية بالصفائح الدموية أن تخفف من التغيرات النسيجية لاعتلال الكلى السكري في ذكور الفئران البيضاء.